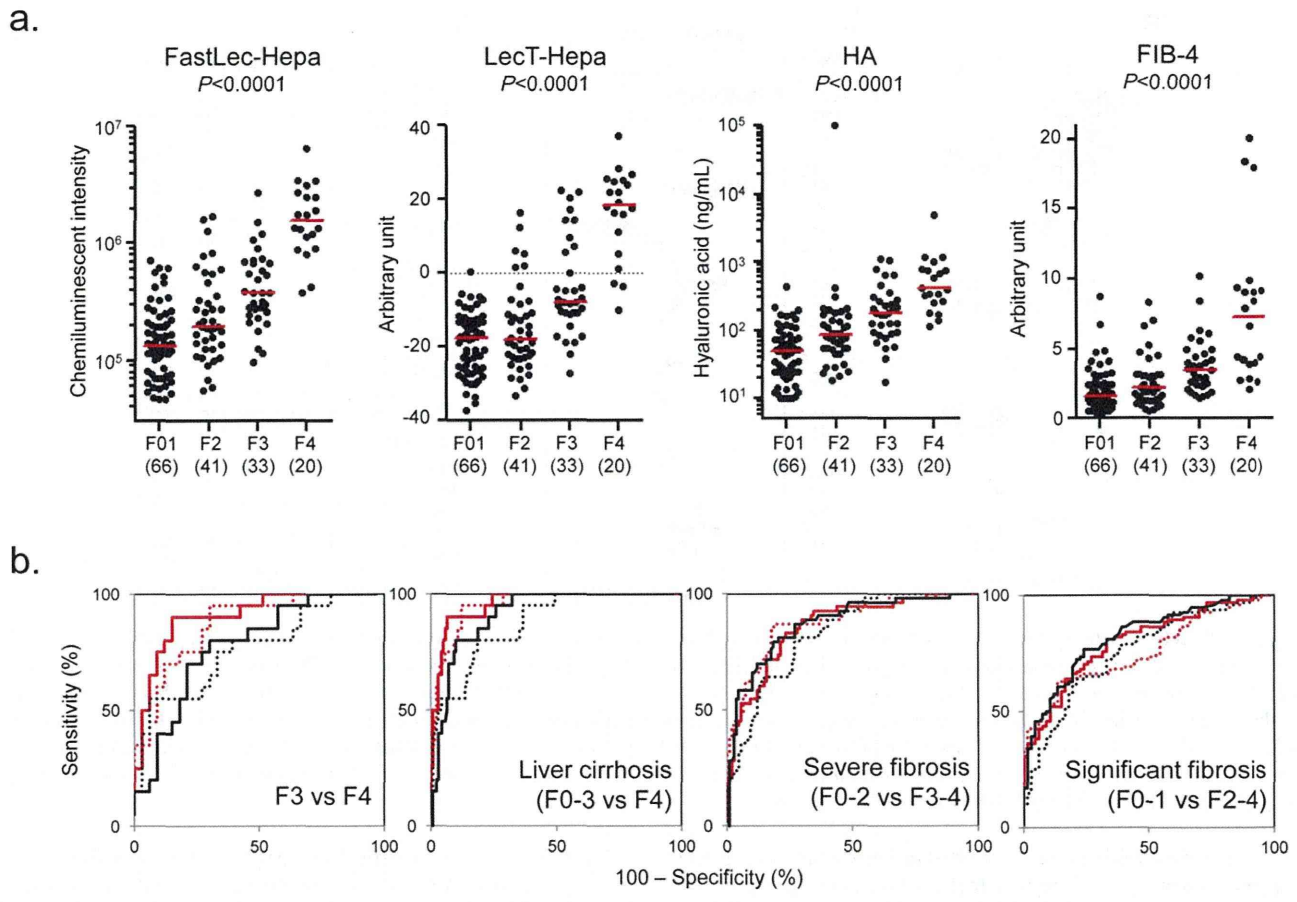

Figure 4 | Comparison of diagnostic performance of FastLec-Hepa, LecT-Hepa, HA, and FIB-4. (a) Scatterplots of the data obtained with FastLec-Hepa, LecT-Hepa, HA, and FIB-4 against the fibrosis score. Red horizontal lines represent the median. Correlation of the data with the progression of fibrosis was evaluated as significant differences in the medians relative to the fibrosis scores ($P < 0.0001$) by a nonparametric method, the Kruskal–Wallis one-way ANOVA. (b) Area under the receiver-operating characteristic (AUC-ROCs) curves of FastLec-Hepa, LecT-Hepa, HA, and FIB-4 for liver cirrhosis (F3 vs F4 or F0–3 vs F4), severe fibrosis (F0–2 vs F3–4), and significant fibrosis (F0–1 vs F2–4). FastLec-Hepa, LecT-Hepa, HA, and FIB-4 are indicated by a red solid line, red dotted line, black solid line, and black dotted line, respectively.

95%, specificity: 70%, and AUC: 0.87), FIB-4 (sensitivity: 55%, specificity: 94%, and AUC: 0.76), and HA (sensitivity: 80%, specificity: 70%, and AUC: 0.78).

Clinical utility of FastLec-Hepa: quantitative monitoring of antiviral therapy. To assess clinical utility, we examined two types of trials—short-interval evaluation and long-term follow-up—both of which are essential for following the patients receiving PEG-interferon-α and ribavirin therapy. For the first trial, we enrolled 41 patients with CHC who had previously undergone 48 weeks of therapy at Hokkaido University Hospital. According to the definition described in the **Methods**, 26 and 15 of them were judged as SVR and NVR/relapse (non-SVR), respectively. For each patient, we performed FastLec-Hepa on serum samples, which were collected just before treatment (Pre) and within a short period (12–22 weeks) after treatment (Post) (**Fig. 5a**). We found a marked decrease from Pre to Post counts ($P = 0.0061$) in SVR patients, but no apparent change for non-SVR patients ($P = 0.9780$) (**Fig. 5b**). Specifically, a median percent decrease of 31% was found for SVR patients (median Pre-count of 161,053 and median Post-count of 110,739), while the level for non-SVR patients was essentially constant. These results show that the assay can evaluate the effect of therapy within a short period after treatment. This is an important advance, because the ALT levels of non-SVR, as well as SVR, are mostly decreased into the range of 10–64 IU/ml during this period (**Fig. 5c**)[5]. In fact, changes in the FastLec-Hepa counts did not correlate with those in the ALT counts (**Supplementary Fig. 13**), thereby invalidating ALT-dependent fibrosis assays, including FIB-4 (**Fig. 5d**).

In support of our finding that the FastLec-Hepa counts correlate excellently with the stage of fibrosis, we found a strong correlation between the histopathological scores and the median of the $\log_{10}$[FastLec-Hepa] counts (**Fig. 5e**). These correlations were approximated to two linear equations: $y = 0.23x + 4.9$ for F0 to F3, and $y = 0.58x + 3.8$ for F3 to F4 histology. This means that FastLec-Hepa can reliably reproduce the assessment of therapeutic effects, which were previously drawn from histopathological scoring[9]. Indeed, the median changes in fibrosis obtained by FastLec-Hepa analysis were about −0.295 stages/year for SVR and 0.010 stages/year for non-SVR (**Fig. 5f**). These data were consistent with the rate of fibrosis progression and regression determined by Shiratori *et al*[9].

For the second trial, we enrolled 6 HCV patients (SVR = 3 and non-SVR = 3) with advanced fibrosis who completed 48 weeks of therapy at Nagoya City University Hospital. Sera were collected before therapy and at 0, 1, 3, and 5 years after the end of therapy (see **Fig. 5g**). FastLec-Hepa counts in SVR patients gradually decreased and reached below the median of F0 patients within 3 years. However, those in non-SVR patients remained above the median for F3 patients during the follow-up period (**Fig. 5h**).

Table 1 | Diagnostic performance of fibrosis markers

n = 160	FIB-4	HA	LecT-Hepa	FastLec-Hepa
a) Significant fibrosis (F0–1 vs F2–4)				
AUC	0.76	0.82	0.76	0.79
(95% CI)	(0.68–0.83)	(0.76–0.89)	(0.69–0.83)	(0.72–0.86)
Diagnostic sensitivity (%)	64	77	63	81
Diagnostic specificity (%)	79	76	86	67
Youden's index (%)	43	52	49	48
b) Severe fibrosis (F0–2 vs F3–4)				
AUC	0.83	0.87	0.88	0.84
(95% CI)	(0.76–0.89)	(0.81–0.93)	(0.82–0.93)	(0.77–0.91)
Diagnostic sensitivity (%)	81	81	87	83
Diagnostic specificity (%)	71	79	81	77
Youden's index (%)	52	61	68	60
c) Liver cirrhosis (F0–3 vs F4)				
AUC	0.88	0.91	0.95	0.96
(95% CI)	(0.80–0.95)	(0.86–0.96)	(0.92–0.99)	(0.93–0.99)
Diagnostic sensitivity (%)	80	80	95	90
Diagnostic specificity (%)	81	90	88	94
Youden's index (%)	61	70	83	84
d) Liver cirrhosis (F3 vs F4)				
AUC	0.76	0.78	0.87	0.91
(95% CI)	(0.63–0.90)	(0.65–0.90)	(0.77–0.97)	(0.82–0.99)
Diagnostic sensitivity (%)	55	80	95	90
Diagnostic specificity (%)	94	70	70	85
Youden's index (%)	49	50	65	75

Interestingly, HCC had developed in two non-SVR patients whose FastLec-Hepa counts remained above the median of F4 patients throughout. Other fibrosis indices, such as FIB-4 and biochemical parameters (ALT and AST), did not distinguish between SVR and non-SVR or appear to predict this occurrence (**Fig. 5i-k**).

Discussion

We have described the development and use of a fully automated, glycan-based immunoassay termed FastLec-Hepa, for the evaluation of liver fibrosis. A high degree of reliability in the quantitative aspects of this method should establish it as a clinically significant test,

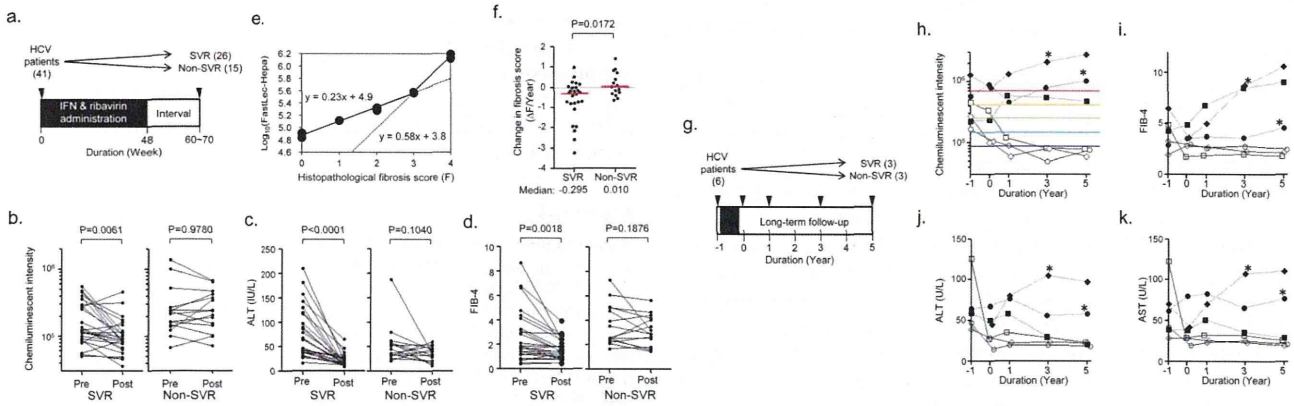

Figure 5 | Evaluation of the curative effect of interferon therapy by FastLec-Hepa. (a) Validation of FastLec-Hepa in short-interval evaluation. The numbers in parentheses represent the number of patients participated in this experiment. Arrowheads indicate the timing of blood collection. At week 0, blood was collected immediately before the treatment. Black box indicates the period of PEG-interferon-α and ribavirin therapy. Changes in the FastLec-Hepa counts (b), ALT (c), and the FIB-4 index (d) in patients with sustained virologic response (SVR) and relapse/nonresponders (non-SVR) during interferon therapy. The *P*-value was determined by a nonparametric method, the Wilcoxon matched pairs signed-rank test. (e) Dot-plot representation of the histopathological fibrosis score and the medians of FastLec-Hepa counts. Best-fit linear curves were calculated in Excel 2007 (Microsoft) allowing conversion of the FastLec-Hepa counts into fibrosis score. (f) Yearly changes in the converted fibrosis score. Changes for patients with SVR and non-SVR are indicated in the dot plots. Red horizontal lines represent the median. The *P*-value was determined by the Mann–Whitney *U* test. (g) Validation of FastLec-Hepa in long-term follow-up. The numbers in parentheses represent the number of patients participated in this experiment. Arrowheads indicate the timing of blood collection. At year -1 and 0, the blood was collected immediately before and after the treatment, respectively. Black box indicates the period of PEG-interferon-α and ribavirin therapy. Yearly changes of FastLec-Hepa counts (h), FIB-4 index (i), ALT (j), and AST (k) in individual patients after therapy. The five colored lines in (h) represent the median values obtained for each fibrosis stage (red, F4; orange, F3; green, F2; cyan, F1; blue, F0). Closed and opened symbols indicate the data obtained from non-SVR and SVR patients, respectively. * indicates the period when the development of HCC was found.

particularly for revealing and managing patients at a high risk of progression to liver complications such as HCC and related life-threatening events. The most striking advantage of FastLec-Hepa is not only its simplicity but also its capacity to provide fibrosis read-outs that are not influenced by fluctuations in the ALT value or inflammation, both of which can cause falsely high estimates in most of the other fibrosis tests available[10]. In fact, our study has illustrated robust capacity of FastLec-Hepa to evaluate the effects of antiviral therapy and subsequent disease progression in both the short and long term.

Many retrospective and prospective studies have demonstrated that achieving SVR through the PEG-interferon-α/ribavirin treatment significantly reduces liver-related morbidity and mortality (i.e., hepatic decompensation, HCC, and liver-related death)[28–30]. As this combination therapy is effective in only about 50% of patients with HCV genotype 1, new agents[1] and targets[31] for antiviral treatments of HCV have been developed to achieve SVR more effectively after the therapy. Long-term follow-ups often show that the risk of disease progression is significantly high in patients with non-SVR after PEG-interferon-α/ribavirin treatment. Furthermore, the development of HCC in patients with SVR remains at a significant cumulative rate (2%)[28,30,32,33]. For these reasons, a new data-mining model using individual factors (age, platelet count, serum albumin and AST) was developed recently to identify patients at a high risk of HCC development[34]. This is, however, a statistical procedure for estimating the chance of disease progression, and there is not a direct evaluation of fibrosis. In the present report, we performed a long-term retrospective study with serially collected sera from SVR and non-SVR patients, in which we showed the potential use of FastLec-Hepa for improved prognostic accuracy. Indeed, recent advances in the development of antifibrotic agents lead us to expect the therapeutic elimination of health risks associated with HCC and decompensation[35]. Moreover, we expect that FastLec-Hepa will be proved for its usefulness in rapid evaluation of progression and regression of fibrosis in clinical trials of newly developed antifibrotic agents. Hence, FastLec-Hepa should be very useful for fibrosis stage screening and evaluation of disease progression in untreated individuals or patients under or after treatment, as well as evaluation of the most recently developed drugs.

It is important to note that FastLec-Hepa has many merits, including speed (possibly 1,000 assays per day) and full automation for measurement of a serological glycobiomarker: these attributes will enable retrospective studies with valuable serum specimens that have been collected previously. In addition, our recently developed calibrator for FastLec-Hepa will improve traceability and enable simultaneous assay and data storage in multiple diagnostic facilities. The data obtained with diluted serum samples demonstrated a high level of assay reproducibility and a very favorable linear detection range (**Supplementary Fig. 14**). Furthermore, we found an excellent agreement between assay values for serum and plasma prepared simultaneously from the same patient. Presently, we have about 10,000 sera and plasma available with detailed clinical notes collected in more than 10 facilities in Japan, and a series of retrospective studies is under way. We will shortly conclude licensing of our system for clinical implementation, based largely on the trials of the present study. In contrast to this, the majority of recent noninvasive techniques are currently shifting to physical measurements such as FibroScan, acoustic radiation force impulse[36] and real-time strain elastography[37]. Any on-site assay of large numbers of blood samples should provide a diagnostic value comparable to that of FibroTest, and a direct comparison in the same patient group will be necessary to evaluate this. We note here that according to a recent statistical validation method[38], predicted AUC of the diagnostic value of FibroTest for detection of advanced fibrosis in our sample set (DANA score = 1.81) was approximately 0.77, which was comparable to the AUC of FastLec-Hepa we obtained (0.79).

FastLec-Hepa has adopted a new paradigm for clinical diagnosis, "glyco-diagnosis", which is based on the quantity and quality of protein glycosylation patterns that well indicate disease progression. To detect such changes in glycosylation by conventional methods (e.g., mass spectrometry, liquid chromatography, or capillary electrophoresis), it is absolutely necessary to liberate the glycans of interest from their protein linkages[15,17,39]. It is possible to employ an alternative technology, which is based on a lectin–antibody sandwich immunodetection system for intact glycoproteins bearing disease-specific glyco-alterations. Such assays have been used to detect changes in fucosylation of *N*-linked glycans, which are associated with liver disease. However, in the present study, fucose-binding lectins were classified as "high noise" (**Fig. 2b**), and thus an enrichment of the target protein was the essential process in the assay. Lectin-overlay detection is performed typically after on-plate enrichment of the target glycoproteins by an immobilized antibody. In such cases, detection relies on a low avidity (high dissociation rate) between the captured glycoprotein and the overlaid lectin probe (see *right* of **Supplementary Fig. 3b**). These kinetic considerations essentially eliminate the use of an automated bedside clinical chemistry analyzer. Even though a fucose-binding lectin was immobilized on the beads (see *left* of **Supplementary Fig. 3b**), it still remains a problem for reliable quantitation by autoanalyzer. Our previous system LecT-Hepa[16,18,19,26], which detects the level of fucosylated α1-acid glycoprotein, requires enrichment of the protein prior to the assay.

In the present study, we have developed a strategy to overcome these problems in glyco-diagnosis associated with clinical implementation, and realized a rapid "on-site diagnosis" system (17 min, within the minimum time required for single assay by HISCL), based on analysis of a glycomarker (**Supplementary Fig. 1**). The strategy for selecting the most robust lectin led us to WFA, and away from the use of fucose-binding lectins, for the direct measurement system (**Fig. 2**). The diagnostic utility of M2BP, a protein resembling "sweet-doughnut"[20], brought a favorable density and orientation of the disease-related glycan on the homomultimer. These characteristic structures resulted in a major increase in the avidity of M2BP for the plated WFA. The resulting glycan–lectin interaction, which is remarkably strong and specific, made it possible to develop the rapid and highly sensitive assay (see *left* of **Supplementary Fig. 3b**). We believe that this unique strategy will revolutionize the use of glyco-diagnosis in clinical medicine and potentially provide a framework for the development of a new generation of biomarker assays.

Methods

Patient samples, biochemical parameters and indices. Patients with chronic hepatitis were enrolled at Nagoya City University Hospital and Hokkaido University Hospital. Healthy volunteers as the controls were randomly selected in Nagoya City University Hospital (70 individuals) and AIST (48 individuals). The institutional ethics committees at Nagoya City University Hospital, Hokkaido University Hospital, and AIST approved this study, and informed consent for the use of their clinical specimens was obtained from all participants before the collection. In addition, we used 1,000 serum samples from virus-negative Caucasians as the normal population, which were purchased from Complex Antibodies Inc. (Fort Lauderdale, FL) and collected under IRB-approved collection protocols. Fibrosis was graded in the patients according to the histological activity index (HAI) using biopsy or surgical specimens. Biopsy specimens were classified as follows: F0, no fibrosis; F1, portal fibrosis without septa; F2, few septa; F3, numerous septa without cirrhosis; and F4, cirrhosis. The three diagnostic targets in this study were defined as significant fibrosis: F2+F3+F4; severe fibrosis: F3+F4; and cirrhosis: F4. Hepatic inflammation was also assessed according to the HAI, as follows: A0, no activity; A1, mild activity; A2, moderate activity; and A3, severe activity. Cirrhosis was confirmed by ultrasonography (coarse liver architecture, nodular liver surface, and blunt liver edges), evidence of hypersplenism (splenomegaly on ultrasonography) and/or a platelet count of $< 100{,}000/mm^3$. Virological responses during PEG-interferon-α and ribavirin therapy were defined as follows[5]: SVR, absence of HCV RNA from serum 24 weeks following discontinuation of therapy; nonresponder, failure to clear HCV RNA from serum after 24 weeks of therapy; relapse, reappearance of HCV RNA in serum after therapy was discontinued. For all patients, age and sex were recorded and serum levels of the following were analyzed: aspartate aminotransferase (AST), alanine aminotransferase (ALT), γ-glutamyltransferase (GGT), total bilirubin,

albumin, cholinesterase, total cholesterol, platelet count (PLT), hyaluronic acid (HA). The FIB-4 index was calculated as follows: [age (years) × AST (U/L)]/[platelets (10^9/L) × ALT (U/L)$^{1/2}$][26]. Fibrosis-specific glyco-alteration of α1-acid glycoprotein was determined by lectin–antibody sandwich immunoassays with a combination of three lectins (*Datura stramonium* agglutinin (DSA), *Maackia amurensis* leukoagglutinin (MAL), and *Aspergillus oryzae* lectin (AOL))[16]. All assays used an automated chemiluminescence enzyme immunoassay system (HISCL-2000i; Sysmex Co., Kobe, Japan)[18].

Enrichment of M2BP from serum. An automated protein purification system (ED-01; GP BioSciences Ltd., Yokohama, Japan) was used to immunoprecipitate M2BP from serum specimens. In brief, sera (2 μl) were diluted 10-fold with PBS/0.2%(w/v) SDS, heated at 95°C for 20 min, mixed with 10 μl of Triton X-100 in TBS (TBSTx) and injected into a 96-well SUMILON microtiter plate (Sumitomo Bakelite Co., Ltd., Tokyo, Japan). The plate and working reagents, including biotinylated anti-M2BP antibody (10 ng/μl), streptavidin-coated magnetic beads, washing buffer (1% TBSTx) and elution buffer (TBS containing 0.2% SDS), were loaded into the system. This generated 110 μl of purified M2BPs per serum sample (96 samples in 3.5 h).

Western blot analysis. Anti-human M2BP polyclonal antibody was purchased from R&D Systems, Inc. (Minneapolis, MN) and biotinylated with Biotin Labeling Kit – NH_2 (Dojindo Laboratories, Kumamoto, Japan). Purified serum M2BPs were electrophoresed under reducing conditions on 5–20% polyacrylamide gels (DRC, Tokyo, Japan) and transferred to PVDF membranes. After treatment with Block Ace® (DS Pharma Biomedical Co., Ltd., Osaka, Japan), the membranes were incubated with biotinylated anti-M2BP polyclonal antibody, and then with alkaline phosphatase-conjugated streptavidin (1/5000 diluted with TBST; ProZyme, Inc., San Leandro, CA). The membranes were incubated with Western Blue stabilized substrate for alkaline phosphatase (Promega, Madison, WI).

Lectin microarray analysis. Enriched M2BPs were analyzed with an antibody-overlay lectin microarray[24]. Purified protein (14 μl) was diluted to 60 μl with PBS containing 1%(v/v) Triton X-100 (PBSTx); this was applied to a LecChip™ (GP BioSciences Ltd.), which included three spots of 45 lectins in each of seven reaction wells. After incubation for 12 h at 20°C, 2 μl of human serum IgG (10 mg/ml) was added to the reaction solution on each chip and incubated for 30 min. The reaction solution was then discarded, and the chip was washed three times with PBSTx. Subsequently, 60 μl (200 ng) of biotinylated anti-human M2BP in PBSTx was applied to the chip, and incubated for 1 h. After three washes with PBSTx, 60 μl (400 ng) of a Cy3-labeled streptavidin (GE Healthcare, Buckinghamshire, UK) solution in PBSTx was added and incubated for 30 min. The chip was rinsed with PBSTx, scanned with an evanescent-field fluorescence scanner (GlycoStation™ Reader1200; GP BioSciences Ltd.) and analyzed with the Array Pro Analyzer software package, version 4.5 (Media Cybernetics, Inc., Bethesda, MD). The chip was scanned with the gain set to register a maximum net intensity < 40,000 for the most intense spots. The net intensity value for each spot was calculated by subtracting the background value from the signal intensity value. The relative intensity of lectin-positive samples was determined from the ratio of their fluorescence to the fluorescence of the internal-standard lectin, DSA.

Quantitation of *Wisteria floribunda* agglutinin (WFA)-binding M2BP. Serum was pretreated as described above under enrichment of M2BP from serum. Pretreated samples (50 μl) were diluted with an equal volume of starting buffer (0.1%(w/v) SDS in PBSTx), added to the WFA-coated agarose in a microtube (20 μl slurry; Vector Lab., Burlingame, UK), and incubated at 4°C for 5 h with gentle shaking. After centrifugation of the reaction solution at 2000 × *g* for 10 min, the supernatant was removed to a new microtube. The precipitate was suspended in 50 μl of the starting buffer, recentrifuged and this second supernatant combined with the first (designated as path-through fraction **T**). The precipitate was then washed with 200 μl of the starting buffer and the bound glycoproteins were eluted with 60 μl of 200 mM galactosamine/0.02%(w/v) SDS in PBS (designated as elution fraction **E**). M2BP was immunoprecipitated from fractions T and E and examined by electrophoresis under reducing conditions on 5–20% gradient SDS–polyacrylamide gels.

WFA-antibody sandwich ELISA. Flat-bottomed 96-well streptavidin-precoated microtiter plates (Nunc, Int., Tokyo, Japan) were treated with biotinylated WFA (Vector, 250 ng/well) for 1 h at room temperature. The plates were incubated with the diluted serum samples (50 μl) in PBS containing 0.1%(v/v) Tween20 (PBS-t) for 2 h at room temperature and then with 50 ng/well of the anti-human M2BP polyclonal antibody, in PBS-t for 2 h at room temperature. The plates were washed extensively and then incubated with 50 μl of horseradish peroxidase (HRP)-conjugated anti-mouse IgG (Jackson ImmunoResearch Laboratories Inc., Philadelphia, PA) at 1:10,000 in PBS-t for 1 h at room temperature. The substrate 3,3′,5,5′-tetramethylbenzidine (Thermo Fisher Scientific, Fremont, CA) solution (100 μl) was added to each well. The enzyme reaction was stopped by adding 100 μl of 1 M sulfuric acid, and the optical density measured at 450 nm.

WFA-antibody sandwich immunoassay by HISCL. The fibrosis-specific form of glycosylated M2BP was measured based on a sandwich immunoassay approach. Glycosylated M2BP was captured by WFA immobilized on magnetic beads, and the bound product was assayed with an anti-human M2BP monoclonal antibody linked to alkaline phosphatase (ALP-αM2BP). Two reagent packs (M2BP-WFA detection pack and a chemiluminescence substrate pack) were loaded in the HISCL. The detection pack comprised three reagents: a reaction buffer solution (R1), a WFA-coated magnetic beads solution (R2) and an ALP-αM2BP solution (R3). The chemiluminescence substrate reagent pack contained a CDP-Star substrate solution (R4) and a stopping solution (R5). Typically, serum (10 μl) was diluted to 60 μl with R1 and then mixed with R2 (30 μl). After the binding reaction, R3 (100 μl) was added to the reaction solution. The resultant conjugates were magnetically separated from unbound components, and mixed well with R4 (50 μl) and R5 (100 μl) before reading of the fluorescence. The chemiluminescent intensity was acquired within a period of 17 min in the operation described above. The reaction chamber was kept at 42°C throughout.

Statistics. Statistical analyses and graph preparation used Dr. SPSS II Windows software (SPSS Co., Tokyo, Japan), GraphPad Prism 5.0 (GraphPad Software Inc., La Jolla, CA), and Windows Excel 2007. This facilitated selection of the optimal lectin for analysis of fibrosis and a comparison of the diagnostic value of other serological fibrosis markers and indices. Because the data distribution for each parameter was non-Gaussian, the *P*-values were determined by nonparametric tests, such as the Mann–Whitney *U* test and Wilcoxon signed-rank test. Correlations with liver fibrosis were estimated as the significance of differences among the staging groups (F0–1, F2, F3, and F4) determined by Kruskal–Wallis nonparametric one-way analysis of variance. To assess classification efficiencies for detecting significant fibrosis, severe fibrosis and cirrhosis, the receiver-operating characteristic (ROC) curve analysis was also carried out to determine the area under the curve (AUC) values. Cutoff values obtained from Youden's index were used to classify patients. Diagnostic accuracy was expressed in terms of specificity, sensitivity and AUC.

1. "Nature Outlook Hepatitis C" edited by Brody, H. *et al. Nature* **474**, S1–S21 (2011).
2. Ge, D. *et al.* Genetic variation in IL28B predicts hepatitis C treatment-induced viral clearance. *Nature* **461**, 399–401 (2009).
3. Suppiah, V. *et al.* IL28B is associated with response to chronic hepatitis C interferon-alpha and ribavirin therapy. *Nat. Genet.* **41**, 1100–1104 (2009).
4. Tanaka, Y. *et al.* Genome-wide association of IL28B with response to pegylated interferon-alpha and ribavirin therapy for chronic hepatitis C. *Nat. Genet.* **41**, 1105–1109 (2009).
5. Ghany, M. G., Strader, D. B., Thomas, D. L. & Seeff, L. B. Diagnosis, management, and treatment of hepatitis C: an update. *Hepatology* **49**, 1335–1374 (2009).
6. Afdhal, N. H. *et al.* hepatitis C pharmacogenetics: state of the art in 2010. *Hepatology* **53**, 336–345 (2011).
7. Peng, C. Y., Chien R. N. & Liaw, Y. N. Hepatitis B virus-related decompensated liver cirrhosis: benefits of antiviral therapy. *J. Hepatol.* **57**, 442–450 (2012).
8. Chang, T. T. *et al.* Long-term entecavir therapy results in the reversal of fibrosis/cirrhosis and continued histological improvement in patients with chronic hepatitis B. *Hepatology* **52**, 886–893 (2010).
9. Shiratori, Y. *et al.* Histologic improvement of fibrosis in patients with hepatitis C who have sustained response to interferon therapy. *Ann. Intern. Med.* **132**, 517–524 (2000).
10. Castera, L. Non-invasive assessment of liver fibrosis in chronic hepatitis C. *Hepatol. Int.* **5**, 625–634 (2011).
11. Imbert-Bismut, F. *et al.* Biochemical markers of liver fibrosis in patients with hepatitis C virus infection: a prospective study. *Lancet* **357**, 1069–1075 (2001).
12. Calès, P. *et al.* A novel panel of blood markers to assess the degree of liver fibrosis. *Hepatology* **42**, 1373–1381 (2005).
13. Castera, L. *et al.* Prospective comparison of two algorithms combining non-invasive methods for staging liver fibrosis. *J. Hepatol.* **52**, 191–198 (2010).
14. Boursier, J. *et al.* Comparison of eight diagnostic algorithm for liver fibrosis in hepatitis C: new algorithms are more precise and entirely noninvasive. *Hepatology* **55**, 58–67 (2012).
15. Callewaert, N. *et al.* Noninvasive diagnosis of liver cirrhosis using DNA sequencer-based total serum protein glycomics. *Nat. Med.* **10**, 429–434 (2004).
16. Kuno, A. *et al.* Multilectin assay for detecting fibrosis-specific glyco-alteration by means of lectin microarray. *Clin. Chem.* **57**, 48–56 (2011).
17. Vanderschaeghe, D. *et al.* High-throughput profiling of the serum N-glycome on capillary electrophoresis microfluidics systems: toward clinical implementation of GlycoHepatoTest. *Anal. Chem.* **82**, 7408–7415 (2010).
18. Kuno, A. *et al.* LecT-Hepa: A triplex lectin-antibody sandwich immunoassay for estimating the progression dynamics of liver fibrosis assisted by a bedside clinical chemistry analyzer and an automated pretreatment machine. *Clin. Chim. Acta* **412**, 1767–1772 (2011).
19. Du, D. *et al.* Comparison of LecT-Hepa and FibroScan for assessment of liver fibrosis in hepatitis B virus infected patients with different ALT levels. *Clin. Chim. Acta* **413**, 1796–1799 (2012).
20. Sasaki, T., Brakebusch, C., Engel, J. & Timpl, R. Mac-2 binding protein is a cell-adhesive protein of the extracellular matrix which self-assembles into ring-like structures and binds beta1 integrins, collagens and fibronectin. *EMBO J.* **17**, 1606–1613 (1998).
21. Iacovazzi, P. A. *et al.* Serum 90K/MAC-2BP glycoprotein in patients with liver cirrhosis and hepatocellular carcinoma: a comparison with alpha-fetoprotein. *Clin. Chem. Lab. Med.* **39**, 961–965 (2001).

22. Artini, M. *et al.* Elevated serum levels of 90K/MAC-2 BP predict unresponsiveness to alpha-interferon therapy in chronic HCV hepatitis patients. *J. Hepatol.* **25**, 212–217 (1996).
23. Cheung, K. J. *et al.* The HCV serum proteome: a search for fibrosis protein markers. *J. Viral. Hepat.* **16**, 418–429 (2009).
24. Kuno, A. *et al.* Focused differential glycan analysis with the platform antibody-assisted lectin profiling for glycan-related biomarker verification. *Mol. Cell. Proteomics* **8**, 99–108 (2008).
25. Kuno, A. *et al.* Evanescent-field fluorescence-assisted lectin microarray: a new strategy for glycan profiling. *Nat. Met.* **2**, 851–856 (2005).
26. Vallet-Pichard, A. *et al.* FIB-4: an inexpensive and accurate marker of fibrosis in HCV infection. Comparison with liver biopsy and fibrotest. *Hepatology* **46**, 32–36 (2007).
27. Ito, K. *et al.* LecT-Hepa, a glyco-marker derived from multiple lectins, as a predictor of liver fibrosis in chronic hepatitis C patients. *Hepatology* **56**, 1448–1456 (2012).
28. Bruno, S. *et al.* Sustained virological response to interferon-α is associated with improved outcome in HCV-related cirrhosis: A retrospective study. *Hepatology* **45**, 579–587 (2007).
29. Cardoso, A.-C. *et al.* Impact of peginterferon and ribavirin therapy on hepatocellular carcinoma: Incidence and survival in hepatitis C patients with advanced fibrosis. *J. Hepatol.* **52**, 652–657 (2010).
30. Morgan, T. R. *et al.* Outcome of sustained virological responders with histologically advanced chronic hepatitis C. *Hepatology* **52**, 833–844 (2010).
31. Lupberger, J. *et al.* EGFR and EphA2 are host factors for hepatitis C virus entry and possible targets for antiviral therapy. *Nat. Med.* **17**, 589–595 (2011).
32. Iwasaki, Y. *et al.* Risk factors for hepatocellular carcinoma in hepatitis C patients with sustained virologic response to interferon therapy. *Liver Int.* **24**, 603–610 (2004).
33. Ikeda, K. *et al.* Anticarcinogenic impact of interferon on patients with chronic hepatitis C: A large-scale long-term study in a single center. *Intervirology* **49**, 82–90 (2006).
34. Kurosaki, M. *et al.* Data mining model using simple and readily available factors could identify patients at high risk for hepatocellular carcinoma in chronic hepatitis C. *J. Hepatol.* **56**, 602–608 (2012).
35. Schuppan, D. & Pinzani, M. Anti-fibrotic therapy: lost in translation? *J. Hepatolol.* **56**, S66–74 (2012).
36. Rizzo, L. *et al.* Comparison of transient elastography and acoustic radiation force impulse for non-invasive staging of liver fibrosis in patients with chronic hepatitis C. *Am. J. Gastroenterol.* **106**, 2112-2120 (2011).
37. Ferraioli, G. *et al.* Performance of real-time sitrain elastography, transient elastgraphy, and aspartate-to-platelet ration index in the assessment of fibrosis in chronic hepatitis C. *AJR Am. J. Roentgenol.* **199**, 19–25 (2012).
38. Poynard, T. *et al.* Standardization of ROC curve areas for diagnostic evaluation of liver fibrosis markers based on prevalences of fibrosis stages. *Clin. Chem.* **53**, 1615–1622 (2007).
39. Nishimura, S. Toward automated glycan analysis. *Adv. Carbohydr. Chem. Biochem.* **65**, 219–271 (2011).

Acknowledgments

This work was supported in part by a grant from New Energy and Industrial Technology Development Organization of Japan. We thank H. Ozaki, H. Shimazaki, S. Unno, K. Saito, M. Sogabe, Y. Kubo, J. Murakami, S. Shirakawa, T. Fukuda (AIST), and H. Naganuma (NCU) for technical assistance. We also thank A. Togayachi, T. Sato, H. Kaji, J. Hirabayashi, H. Tateno, A. Takahashi (AIST) and C. Tsuruno, S. Nagai and Y. Takahama (Sysmex Co.) for critical discussion.

Author contributions:

A.K. conceived and designed the study, performed most of the biochemical experiments, analyzed data and wrote the paper with comments from Y.T., M.M. and H.N.; Y.I. conceived and designed the study, performed the sample pre-treatment for the assay, and analyzed data; Y.T., K.I., M.M., and S.H collected clinical samples, designed the validation study, and analyzed data; A.M. and S.S. performed the biochemical experiments including lectin microarray analysis and analyzed data; M.S. and M.K. performed staging of biopsy specimens by histological activity index (HAI); H.N. conceived and designed the study, and supervised all aspects of the work; and all authors discussed the results and implications, and commented on the paper.

Additional information

Supplementary information accompanies this paper at http://www.nature.com/scientificreports

Competing financial interests: The authors declare no competing financial interests.

How to cite this article: Kuno, A. *et al.* A serum "sweet-doughnut" protein facilitates fibrosis evaluation and therapy assessment in patients with viral hepatitis. *Sci. Rep.* 3, 1065; DOI:10.1038/srep01065 (2013).

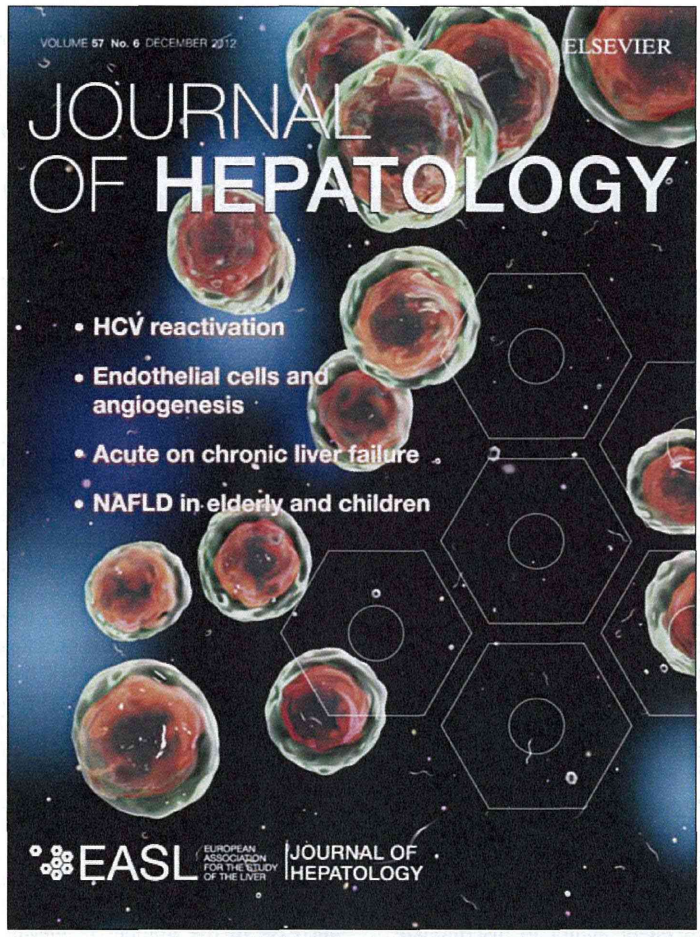

Research Article

EASL EUROPEAN ASSOCIATION FOR THE STUDY OF THE LIVER | JOURNAL OF HEPATOLOGY

Prognostic significance of a combination of pre- and post-treatment tumor markers for hepatocellular carcinoma curatively treated with hepatectomy

Hidenori Toyoda[1,*], Takashi Kumada[1], Toshifumi Tada[1], Takuro Niinomi[1], Takanori Ito[1], Yuji Kaneoka[2], Atsuyuki Maeda[2]

[1]*Department of Gastroenterology, Ogaki Municipal Hospital, Ogaki, Japan;* [2]*Department of Surgery, Ogaki Municipal Hospital, Ogaki, Japan*

Background & Aims: Previous studies reported that the combination of three tumor markers for hepatocellular carcinoma (HCC), alpha-fetoprotein (AFP), *Lens culinaris* agglutinin-reactive AFP (AFP-L3), and des-gamma-carboxy prothrombin (DCP), has the ability to discriminate survival among patients with HCC. In those studies, however, the study population included all patients with various treatment modalities, and tumor markers were measured only before treatment. We investigated the prognostic value of a combination of these tumor markers for HCC, measured before and after treatment, on survival and recurrence in patients treated with hepatectomy.

Methods: A total of 173 patients who underwent hepatectomy for primary, non-recurrent HCC were analyzed. Tumor characteristics, postoperative survival, and recurrence rates were compared according to the number of elevated tumor markers measured before and after treatment.

Results: The correlation between the number of elevated tumor markers before treatment and tumor size, rate of portal vein invasion, and tumor differentiation, respectively, was stronger than that between the number of elevated tumor markers after treatment. In contrast, the number of elevated tumor markers after treatment displayed an excellent ability to discriminate post-treatment survival and recurrence rates compared to that before treatment, and was an independent factor associated with survival and recurrence in multivariate analysis.

Conclusions: The combination of tumor markers measured after hepatectomy has a better discriminatory ability for postoperative survival and recurrence in HCC patients treated with hepatectomy in comparison to the combination of tumor markers measured before treatment.

Keywords: Hepatocellular carcinoma; Tumor markers; Survival; Recurrence; Curative hepatectomy.

Received 5 April 2012; received in revised form 11 July 2012; accepted 11 July 2012; available online 20 July 2012

* Corresponding author. Address: Department of Gastroenterology, Ogaki Municipal Hospital, 4-86 Minaminokawa, Ogaki, Gifu 503-8502, Japan. Tel.: +81 584 81 3341; fax: +81 584 75 5715.

E-mail address: hmtoyoda@spice.ocn.ne.jp (H. Toyoda).

Abbreviations: HCC, hepatocellular carcinoma; AFP, alpha-fetoprotein; AFP-L3, *Lens culinaris* agglutinin-reactive fraction of alpha-fetoprotein; DCP, des-gamma-carboxy prothrombin; PIVKA-II, vitamin K absence/antagonist-II; CT, computed tomography; US, ultrasound; MRI, magnetic resonance imaging.

Introduction

Hepatocellular carcinoma (HCC) is the sixth most common cancer worldwide and the third most common cause of cancer-related death [1,2]. In Japan, HCC currently represents the third and fifth most common cause of death from cancer in men and women, respectively, [3]. Presently, three tumor markers specific for HCC are used clinically: alpha-fetoprotein (AFP), *Lens culinaris* agglutinin-reactive fraction of AFP (AFP-L3), and des-gamma-carboxy prothrombin (DCP), which is also known as protein induced by vitamin K absence/antagonist-II (PIVKA-II). The clinical utility of these tumor markers for detection and diagnosis of HCC, for evaluation of tumor progression, and for determination of prognosis has been reported [4–7]. In addition, the combination of these three tumor markers has been indicated as a useful predictor of patient outcome. We previously reported the prognostic significance of the combination of three tumor markers measured at diagnosis on the survival of all patients with HCC [8]. An increase in the number of elevated tumor markers, consisting of AFP, AFP-L3, and DCP, was clearly associated with a decreased survival rate in patients with HCC. In addition, an increase in the number of elevated tumor markers was well correlated with indicators of HCC progression, including the size and number of tumors, and the rate of portal vein invasion. More recently, Kim *et al.* have reported less progression of HCC without the elevation of AFP and DCP, with higher survival rates [9].

However, in these studies, all patients with HCC who underwent various treatment modalities had been included into the study. In addition, the levels of tumor markers were measured at diagnosis and before treatment. The predictive ability of post-treatment *vs.* pretreatment tumor markers has not been evaluated and compared. In the present study, we measured the levels of these three tumor markers both before and after treatment, in patients who underwent hepatectomy with curative intent. We analyzed their relationship with tumor progression, survival, and recurrence after treatment.

Materials and methods

Patients

A total of 828 patients were diagnosed with primary, non-recurrent HCC, between January 2001 and December 2010 at Ogaki Municipal Hospital. Of these

Cancer

patients, 264 were treated with hepatectomy. Stored serum samples were available for measurement of the levels of three tumor markers, AFP, AFP-L3, and DCP, before and after hepatectomy in 173 patients. Decisions regarding each patient's course of treatment were made based on the treatment guidelines for HCC in Japan [10]. Anatomical hepatectomy was performed in all 173 patients. HCC tumors were resected with ample margins and enucleation of tumors without adequate margins was not performed. The diagnosis of HCC was confirmed by pathologic examination of resected specimens.

One month after hepatectomy, all patients underwent computed tomography (CT) examination of thorax and abdomen to confirm the absence of residual HCC. All patients were followed-up, for a median of 34.2 months (range, 4.3–122.8 months) until March 2012 at our institution, with ultrasound (US) and CT, or US and magnetic resonance imaging (MRI) every 3–6 months. Regular monitoring of the three tumor markers was performed every 3 months. When an elevation of tumor markers was detected, additional imaging examinations (usually CT or MRI) were performed to check for recurrence. If the presence of recurrence was confirmed, patients underwent treatment for recurrent HCC based on treatment guidelines.

The entire protocol was approved by the hospital institutional review board and carried out in compliance with the Helsinki Declaration.

Measurement of hepatocellular carcinoma tumor markers

Pretreatment tumor markers were measured within 1 week before hepatectomy. Post-treatment tumor markers were measured in the serum sample obtained at the first visit, between 1 and 2 months after hepatectomy. The reported half-lives of AFP and AFP-L3 are 4 days [11] and the half-life of DCP is 60 h [12]. Therefore, the values of post-treatment tumor markers were not influenced by pretreatment tumor marker elevations. Measurements of AFP, AFP-L3, and DCP levels were performed with a microchip capillary electrophoresis and liquid-phase binding assay on the μTASWako i30 auto analyzer (Wako Pure Chemical Industries, Ltd., Osaka, Japan) [13]. The cut-off value of 20 ng/ml was used to establish positivity for AFP, as proposed by Oka *et al.* and Koda *et al.* [14,15]. The cut-off value used to establish positivity for AFP-L3 was 5%, based on our previous study [16]. The cut-off value used to establish positivity for DCP was 40 mAU/ml, as proposed by Okuda *et al.* [17]. The number of tumor markers above the cut-off values was calculated as the number of elevated tumors markers, and survival and recurrence rates were analyzed according to the number of elevated tumor markers.

Statistical analyses

Differences in percentages between groups were analyzed with the Chi-square test. Differences in mean quantitative values were analyzed with the Mann–Whitney *U* test. Changes in percentages and quantitative values with the increase in the number of elevated tumor markers were analyzed with the Cochran–Armitage test and the Jonckheere–Terpstra test, respectively. Receiver-operating characteristics analyses were performed to determine the cut-offs of the number of elevated tumor markers in order to evaluate the accuracy of prediction of 1-, 3-, and 5-year survivals and recurrences and compare them with the accuracy of elevation of each tumor marker. The date of hepatectomy was defined as time zero for the calculation of survival and recurrence rates. In the analysis of survival rates, patients who died were non-censored and patients who survived were censored. In the analysis of recurrence rates, patients in whom HCC recurred were non-censored, and those in whom HCC did not recur were censored. The Kaplan–Meier method [18] was used to calculate survival and recurrence rates, and the log-rank test [19] was used to analyze differences in survival and recurrence.

The Cox proportional hazards model [20] was used for multivariate analyses of factors related to survival and recurrence. Variables analyzed included age, sex, Child-Pugh class (A/B), tumor size, number of tumors, differentiation of HCC (well-moderately or poorly), growth pattern (expansive growth/infiltrative growth), macroscopic and microscopic portal vein invasion (absent/present), and number of elevated tumor markers (zero, one, two, or three). Data analyses were performed using JMP statistical software, version 6.0 (Macintosh version; SAS Institute, Cary, NC, USA). All p values were derived from two-tailed tests, with $p < 0.05$ considered to indicate statistical significance.

Results

Characteristics of patients and hepatocellular carcinoma

Table 1 summarizes the pretreatment characteristics of the study patients. This population comprised 136 males and 37 females with a mean age of 67.0 ± 8.8 years. Most (95.4%) patients belonged to Child-Pugh class [21] A. Multiple tumors were present in 16.8% of patients. HCC was well differentiated in 37.0% and portal vein invasion was observed in 23.1% of patients, based on the pathologic examination of resected HCC specimens. Pretreatment AFP, AFP-L3, and DCP were above the specified cut-off levels in 34.7%, 44.5%, and 52.0% of patients, respectively.

Clinical and pathologic characteristics of hepatocellular carcinoma based on a combination of three tumor markers measured before and after hepatectomy

At pretreatment, there were 47 (27.2%) patients with no elevated tumor markers and 57 (32.9%) patients with one, 38 (22.0%) with two, and 31 (17.9%) with three elevated tumor markers. After hepatectomy, 75 (43.3%) patients had no elevated tumor markers, 70 (40.5%) patients had one, 24 (13.9%) had two, and 4 (2.3%) had three elevated tumor markers. Tables 2 shows pretreatment clinical characteristics and pathologic characteristics of the resected HCC specimens according to the number of elevated tumor markers measured before and after hepatectomy. An increase in tumor size was associated with an increase in the number of elevated tumor markers before treatment ($p < 0.0001$). This gradual increase in tumor size according to the number of elevated tumor markers was not observed with post-treatment values ($p = 0.5836$). On pathologic examination, there was a gradual decrease in the rate of well-differentiated HCC ($p < 0.0001$) and of HCC with expansive growth ($p = 0.0010$), and a gradual increase in the rate of HCC with portal vein invasion ($p < 0.0001$) based on the number of elevated tumor markers before treatment. These are not significant when compared with postoperative values (the rate of well-differentiated HCC, $p = 0.3962$, of HCC with expansive growth, $p = 0.3036$, and the rate of HCC with portal vein invasion, $p = 0.0898$).

Post-operative survival rates based on the combination of three tumor markers measured before and after hepatectomy

The survival rates were compared by the elevation of each tumor marker. By comparing tumor markers measured before treatment, we found significant differences in survival rates by elevated AFP, and AFP-L3 levels, but not DCP (Supplementary Fig. 1). By comparing tumor markers measured after treatment, survival rates were significantly lower in patients with elevated AFP, AFP-L3, and DCP levels, respectively (Supplementary Fig. 2). We determined the survival rates of patients after hepatectomy as a function of the number of elevated tumor markers before and after hepatectomy (Fig. 1). The number of elevated tumor markers after treatment provided a better discrimination of survival rates than the number of elevated tumor markers before treatment. The survival rates were higher in patients without elevated tumor markers after treatment, followed by patients with one, two, and three elevated tumor markers, in this order.

We next compared the accuracy of death prediction between each individual tumor marker and the combination of the three (Supplementary Table 1). Higher accuracy in predicting death within 1, 3, and 5 year(s), respectively, was found by combining the three markers than by each individual marker alone.

In multivariate analysis, the number of elevated tumor markers was not associated with specific survival after hepatectomy, when tumor markers measured before treatment were used (Supplementary Table 2). In contrast, it was an independent

Table 1. Characteristics of the study patients (n = 173).

Age (yr); (range)	67.0 ± 8.8 (21-83)
Sex (female/male)	37 (21.4)/136 (78.6)
Etiology (HBV/HCV/HBV+HCV/non-HBV, non-HCV)	29 (16.8)/116 (67.0)/2 (1.2)/26 (15.0)
Child-Pugh class (A/B)	165 (95.4)/8 (4.6)
Albumin (g/dl)	4.02 ± 0.42
Total bilirubin (mg/dl)	0.78 ± 0.34
15-min retention rate of ICG (%)	15.4 ± 7.4
Prothrombin (%)	92.7 ± 14.3
Platelet (x10^3/ml)	144 ± 71
Tumor size (cm); (range)	3.28 ± 2.59 (0.8-16.4)
Number of tumors (n); (range)	1.24 ± 0.56 (1-3)
Single/multiple	144 (83.2)/29 (16.8)
Macroscopic portal vein invasion (absent/present)*	167 (96.5)/6 (3.5)
Microscopic portal vein invasion (absent/present)	133 (76.9)/40 (23.1)
Differentiation (well-/moderately or poorly)	64 (37.0)/109 (63.0)
Growth pattern (expansive growth/infiltrative growth)	151 (87.3)/22 (12.7)
AFP (ng/ml); median (range)	10.9 (0.8-27,242.8)
≥20 ng/ml/<20 ng/ml	60 (34.7)/113 (65.3)
AFP-L3 (%); median (range)	3.9 (0.0-89.7)
≥5%/<5%	77 (44.5)/96 (55.5)
DCP (mAU/ml); median (range)	43.0 (5.0-60,030.0)
≥40 mAU/ml/<40 mAU/ml	90 (52.0)/83 (48.0)

Values are mean ± SD, unless otherwise indicated.
Percentages are given in parentheses, unless otherwise indicated.
HBV, hepatitis B virus; HCV, hepatitis C virus; ICG, indocyanine green test; AFP, alpha-fetoprotein; AFP-L3, *Lens culinaris* agglutinin-reactive AFP; DCP, des-gamma-carboxy prothrombin.
*Evaluated based on imaging findings.

factor associated with survival when the number of elevated tumor markers was replaced by those measured after treatment (Table 3).

Post-treatment recurrence rates based on the combination of three tumor markers measured before and after hepatectomy

The rates of recurrence were compared by the elevation of each tumor marker. In comparisons of tumor markers measured before treatment, we did not find significant differences in recurrence rates by the elevation of AFP and DCP (Supplementary Fig. 3). In comparisons of tumor markers measured after treatment, recurrence rates were significantly higher in patients with elevated AFP, AFP-L3, and DCP levels, respectively (Supplementary Fig. 4). We determined the rates of recurrence in patients, after hepatectomy with curative intent, based on the number of elevated tumor markers before and after hepatectomy (Fig. 2). We did not find any difference in the recurrence rates based on the number of elevated tumor markers measured before treatment. In contrast, higher recurrence rates were associated with an increasing number of elevated tumor markers measured after treatment. Moreover, higher accuracy in prediction of recurrence within 1, 3, and 5 year(s), was found with the combination of these three markers than with each individual marker alone (Supplementary Table 3).

In multivariate analysis, the number of elevated tumor markers was not associated with recurrence after hepatectomy, when tumor markers measured before treatment were used (Supplementary Table 4). In contrast, it was an independent factor associated with recurrence when the number of elevated tumor markers was replaced by those measured after treatment (Table 4).

Discussion

In the present study, we investigated the significance of a combination of three tumor markers for HCC (AFP, AFP-L3, and DCP) measured after treatment *vs.* before treatment, in predicting outcome in patients undergoing hepatectomy with curative intent. Our results demonstrated that the number of elevated tumor markers after treatment had a better discriminatory ability for both survival and recurrence rates after hepatectomy. A gradual decrease in survival rates and an increase in recurrence rates were observed as the number of post-treatment elevated tumor markers increased.

In our previous study of 685 patients with HCC [8], the number of elevated tumor markers measured before treatment was well associated with the progression of HCC and survival rates. In contrast, in the present study, the number of elevated pretreatment tumor markers did not predict survival and recurrence rates, although it was associated with the progression of HCC. This could be due to the fact that the patients analyzed in our previous study underwent various types of treatment according to HCC progression and liver function, while in the present study we focused on HCC patients who underwent hepatectomy with

Table 2. Clinical characteristics of patients with HCC based on the number of positive tumor markers measured (A) before hepatectomy and (B) after hepatectomy (n = 173).

A

	Number of positive tumor markers before treatment			
	0 (n = 47)	1 (n = 57)	2 (n = 38)	3 (n = 31)
Age (yr)	67.1 ± 7.6	67.8 ± 8.0	68.2 ± 8.4	64.2 ± 12.0
Sex (female/male)	6 (12.8)/41 (87.2)	16 (28.1)/41 (71.9)	10 (26.3)/28 (73.7)	5 (16.1)/26 (83.9)
Child-Pugh class (A/B)	46 (97.9)/1 (2.1)	55 (96.5)/2 (3.5)	35 (92.1)/3 (7.9)	29 (93.5)/2 (6.5)
Albumin (g/dl)	4.03 ± 0.32	4.04 ± 0.45	3.96 ± 0.48	4.06 ± 0.43
Total bilirubin (mg/dl)	0.75 ± 0.34	0.77 ± 0.28	0.81 ± 0.39	0.80 ± 0.36
15-min retention rate of ICG (%)	14.9 ± 6.2	16.6 ± 9.1	16.1 ± 6.7	13.1 ± 5.6
Prothrombin (%)	93.1 ± 13.9	90.8 ± 15.6	91.3 ± 11.9	97.2 ± 14.9
Platelet (x10^3/ml)	149 ± 89	140 ± 62	138 ± 70	150 ± 59
Tumor size (cm)[1]	2.25 ± 1.09	2.96 ± 2.02	3.75 ± 2.88	4.87 ± 3.74
Number of tumors (single/multiple)	40 (85.1)/7 (14.9)	50 (87.7)/7 (12.3)	30 (78.9)/8 (21.1)	24 (77.4)/7 (22.6)
Differentiation (well-/moderately or poorly)[2]	26 (55.3)/21 (44.7)	27 (47.4)/30 (52.6)	9 (23.7)/29 (76.3)	2 (6.5)/29 (93.5)
Growth pattern (expansive/infiltrative)[3]	44 (93.6)/3 (6.4)	53 (93.0)/4 (7.0)	34 (89.5)/4 (10.5)	20 (64.5)/11 (35.5)
Capsular formation (absent/present)*	24 (54.5)/20 (45.5)	25 (47.2)/28 (52.8)	10 (29.4)/24 (70.6)	3 (15.0)/17 (85.0)
Capsular infiltration (absent/present)**	11 (55.0)/9 (45.0)	15 (53.6)/13 (46.4)	8 (33.3)/16 (66.7)	6 (35.3)/11 (64.7)
Portal vein invasion (absent/present)***,[4]	44 (93.6)/3 (6.4)	52 (91.2)/5 (8.8)	27 (71.1)/11 (28.9)	10 (32.3)/21 (67.7)

B

	Number of positive tumor markers after treatment			
	0 (n = 75)	1 (n = 70)	2 (n = 24)	3 (n = 4)
Age (yr)	67.7 ± 9.3	66.8 ± 7.9	65.1 ± 10.3	72.0 ± 4.5
Sex (female/male)	14 (18.7)/61 (81.3)	17 (24.3)/53 (75.7)	6 (25.0)/18 (75.0)	0/4 (100.0)
Child-Pugh class (A/B)	73 (97.3)/2 (2.7)	64 (91.4)/6 (8.6)	24 (100.0)/0	4 (100.0)/0
Albumin (g/dl)	4.10 ± 0.41	3.99 ± 0.44	3.88 ± 0.35	4.13 ± 0.39
Total bilirubin (mg/dl)	0.82 ± 0.36	0.73 ± 0.31	0.74 ± 0.31	0.80 ± 0.35
15-min retention rate of ICG (%)	14.6 ± 6.2	16.3 ± 8.8	15.7 ± 6.4	15.5 ± 4.6
Prothrombin (%)	94.4 ± 13.3	90.4 ± 16.1	93.7 ± 12.8	94.8 ± 6.2
Platelet (x10^3/ml)	157 ± 87	136 ± 58	121 ± 52	161 ± 39
Tumor size (cm)	3.33 ± 2.58	2.86 ± 1.93	3.71 ± 3.11	6.90 ± 6.44
Number of tumors (single/multiple)	63 (84.0)/12 (16.0)	61 (87.1)/9 (12.9)	18 (75.0)/6 (25.0)	2 (50.0)/2 (50.0)
Differentiation (well-/moderately or poorly)	30 (40.0)/45 (60.0)	25 (35.7)/45 (64.3)	9 (37.5)/15 (62.5)	0/4 (100.0)
Growth pattern (expansive/infiltrative)	66 (88.0)/9 (12.0)	64 (91.4)/6 (8.6)	18 (75.0)/6 (25.0)	3 (75.0)/1 (25.0)
Capsular formation (absent/present)*	23 (34.8)/43 (65.2)	33 (51.6)/31 (48.4)	6 (33.3)/12 (66.7)	0/3 (100.0)
Capsular infiltration (absent/present)**	20 (46.5)/23 (53.5)	17 (54.8)/14 (45.2)	3 (25.0)/9 (75.0)	0/3 (100.0)
Portal vein invasion (absent/present)***	59 (78.7)/16 (21.3)	59 (84.3)/11 (15.7)	14 (58.3)/10 (41.7)	1 (25.0)/3 (75.0)

[1]p <0.0001 (Jonckheere–Terpstra test); [2,4]p <0.0001; [3]p = 0.0010 (Cochran–Armitage test).
ICG, indocyanine green test.
*Evaluated only in HCC with expansive growth.
**Evaluated only in HCC with capsular formation.
***On pathologic evaluation.
Unless otherwise indicated, values are mean ± SD and percentages are indicated in parentheses.
ICG, indocyanine green test.

curative intent. Recently, Kiriyama *et al.* have investigated the utility of the combination of these three tumor markers measured at diagnosis (before treatment) in predicting outcomes in HCC patients treated with hepatectomy [22]. They have reported that elevation of all three tumor markers (triple positive tumor markers) is associated with invasive tumor growth, and patients